JOURNAL OF THEORETICAL
AND APPLIED MECHANICS
57, 4, pp. 957-972, Warsaw 2019
DOI: 10.15632/jtam-pl/112419

VIBRATION SUPPRESSION OF TRUNCATED CONICAL SHELLS EMBEDDED WITH MAGNETOSTRICTIVE LAYERS BASED ON FIRST ORDER SHEAR DEFORMATION THEORY

Shahin Mohammadrezazadeh, Ali Asghar Jafari
Faculty of Mechanical Engineering, K.N. Toosi University of Technology, Tehran, Iran
e-mail: sh.mrezazadeh@email.kntu.ac.ir; ajafari@knti.ac.ir

Vibration phenomena in mechanical structures including conical shells are usually undesirable. In order to overcome this problem, this study investigates active vibration control of isotropic truncated conical shells containing magnetostrictive actuators. The first-order shear deformation theory and the Hamilton principle are handled to obtain vibration equations. Moreover, a negative velocity feedback control law is used to actively suppress the vibration. The Ritz and modified Galerkin methods are utilized to obtain results of shell vibration. The results are validated by comparison with the results of literature and finite element software. Finally, the effects of control gain value, magnetostrictive layers thickness, isotropic layer thickness, length and semi-vertex angle of the conical shell on vibration suppression characteristics are obtained in details.

Keywords: isotropic truncated conical shell, magnetostrictive layers, active vibration control, first order shear deformation theory, Ritz method, modified Galerkin method

1. Introduction

Vibration control of structures is very important because of damaging effects of vibration to structural systems. In recent years, several materials called smart materials have been used in sensor/actuator applications in order to decrease and suppress vibration. Piezoelectric materials, magnetostrictive materials, electrostrictive materials, shape memory alloys and electro-rheological fluids are all from smart materials (Pradhan and Reddy, 2004). Magnetostrictive materials can serve both as solid-state actuators and as magnetic field sensors (Chopra and Sirohi, 2013). When a magnetic field is applied to these materials, randomly oriented magnetic domains rotate to align themselves along the field (Chopra and Sirohi, 2013). Some magnetostrictive materials such as Terfenol-D exhibit measurable magnetostrictive strains on the order of microstrain ($2000 \cdot 10^{-6}$) (Chopra and Sirohi, 2013). Magnetostrictive materials are found in the form of rods, thin films and powder (Chopra and Sirohi, 2013). These materials usually are ready to assemble into devices without any processing (Chopra and Sirohi, 2013). Magnetostrictive materials are now being used for several applications such as active vibration and noise control of systems, machine tools, servo-valves, hybrid motors, automotive brake systems, micro-positioners, particulate-actuators and sensors (Chopra and Sirohi, 2013 quoted from Hunt, 1953; Goodfriend *et al.*, 1994; Dapino *et al.*, 1999).

Several researchers have used magnetostrictive materials in order to attenuate vibration. Pradhan and Reddy (2004) suppressed natural vibration of laminated composite shell panels using magnetostrictive actuating layers based on the first-order shear deformation shell theory. Kumar *et al.* (2004) used a distributed magnetostrictive layer bonded to a plate to control vibration of the plate based on a negative velocity feedback control approach. Pradhan (2005) applied the Navier solution and the first-order shear deformation shell theory to suppress vibration of the

functionally graded shells with embedded magnetostrictive layers. Oates and Smith (2008) designed a nonlinear control for attenuating structural vibrations via magnetostrictive transducers operating in nonlinear and highly hysteretic operating regimes. Hong (2014) derived vibration and a transient answer of rapid heating on the inner surface of functionally graded material (FGM) circular cylindrical shells which had a magnetostrictive material in their outer layer based on a generalized differential quadrature (GDQ) method. Zhang *et al.* (2015) investigated active vibration damping of a cantilever laminated composite plate with giant magnetostrictive material layers using a nonlinear and coupled constitutive model. Hong (2016) utilized GDQ method to derive computational results of three-layer cross-ply composite magnetostrictive shells under sudden uniform heat persuaded vibration. Ghorbanpour Arani *et al.* (2017) presented a feedback control system for studying the free vibration response of a rectangular plate made of a magnetostrictive material. Trigonometric higher order shear deformation theory was used in that study.

Conical shells are structures which have numerous applications in industry. Several researchers have studied the vibration response of truncated conical shells with various techniques. Irie *et al.* (1984) presented natural frequencies of a truncated conical shell with different boundary conditions. Tong (1994) presented solutions in the form of power series to investigate free vibration of composite laminated conical shells including the transverse shear deformation and the extension-bending coupling. Civalek (2006) used a discrete singular convolution (DSC) algorithm to investigate free vibration of single isotropic and orthotropic conical shells based on Love's first approximation thin shell theory. Li *et al.* (2009) presented the solution for forced vibration of a conical shell by means of the Rayleigh-Ritz method. Jin *et al.* (2014) derived a precise modified Fourier series solution to investigate free vibration of truncated conical shells with general elastic boundary conditions. Firouz-Abadi *et al.* (2014) utilized the Novozhilov theory in order to study free vibration of moderately thick conical shells. Kamarian *et al.* (2016) determined the free vibration solution of carbon nanotube-reinforced composite conical shells by using the GDQ method. Bagheri *et al.* (2017) investigated free vibration of a shear deformable conical shell with an intermediate ring support using the first order shear deformation shell theory. Shakouri and Kouchakzadeh (2017) obtained natural frequencies of generally laminated conical and cylindrical shells under arbitrary boundary conditions using a simple analytical method based on the Donnell thin-walled shell theory. Xie *et al.* (2017) analyzed free and forced vibration of stepped conical shells with general boundary conditions by means of an analytical method. Nasihatgozar and Khalili (2019) obtained vibration and buckling responses of laminated sandwich truncated conical shells with a compressible or incompressible core assuming curvature effects. Sofiyev *et al.* (2017) investigated dynamic instability of functionally graded (FG) truncated conical shells under dynamic axial load using first order shear deformayion theory. Sofiyev (2018) investigated free vibration of laminated orthotropic conical shells based on a modified first order shear deformation theory. Sofiyev and Kuruoglu (2018) extracted excitation frequencies of parametric vibration of laminated non-homogeneous orthotropic conical shells under axial load periodically varying with time based on the classical shell theory. Mehditabar *et al.* (2018) derived the vibration response of an antisymmetric angle-ply laminated conical shell based on a transverse shear deformation theory.

It can be concluded from literature that active vibration control of isotropic truncated conical shells based on the first order shear deformation theory should be considered. Because of the importance of damping of undesirable vibration of the conical shells, this paper investigates the active vibration control of isotropic truncated conical shells with a pair of magnetostrictive layers embedded into the host material under simply supported boundary conditions based on the first order shear deformation theory. Hamilton's principle is used for obtaining vibration equations. Then, kinematics of the shell, which is described in the form of partial differential equations, is converted to ordinary differential equations using the Ritz and modified Galerkin

methods. The vibration responses of the shell are controlled using a velocity feedback control law. The influences of bounding values of longitudinal and circumferential wave numbers on the convergence of the responses are studied. The validation of the results is investigated by comparison with the results published in literature and also finite element software results, and very good agreement is observed. The effects of the control gain value, magnetostrictive layers thickness, isotropic layer thickness, length and semi-vertex angle of the conical shell on the vibration suppression characteristics are discussed in details.

2. Basic formulations

An isotropic truncated conical shell with length L, small edge radius R_1, large edge radius R_2 and semi-vertex angle α under simply supported boundary conditions is considered here. This shell is embedded with two magnetostrictive layers on its inner and outer surfaces. The total thickness of the shell is h_T while isotropic and magnetostrictive layers thicknesses are denoted by h and h_m, respectively. The schematic of the considered conical shell is shown in Fig. 1. The coordinate system x-θ-z with the origin point at the small edge on the mid-surface of the shell is considered. The x-coordinate is assumed along the shell generator while θ and z demonstrate the circumferential and thickness coordinates, respectively.

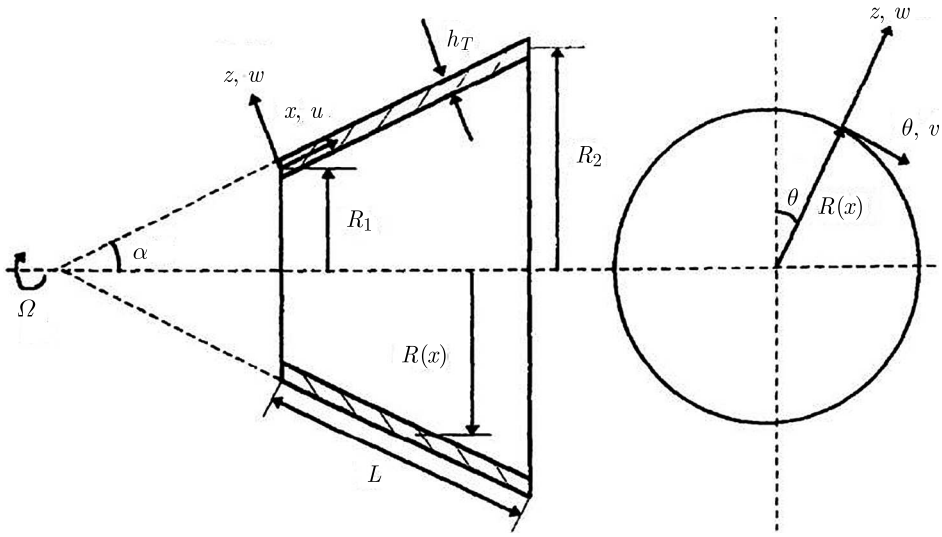

Fig. 1. Schematic of the conical shell with reference coordinates (Lam and Hua, 1997)

Considering the first order shear deformation shell theory (FSDT), the displacement field is defined in the following form (Rao, 2007)

$$u = u_0 + z\psi_x \qquad v = v_0 + z\psi_\theta \qquad w = w_0 \tag{2.1}$$

In Eq. (2.1), u, v and w demonsrate the displacements along x, θ and z coordinates for a randomly selected point while u_0, v_0 and w_0 refer to the shell middle surface displacements along x, θ and z directions. In addition, ψ_x and ψ_θ illustrate the total angular rotations of the normal to the mid-surface about θ and x axes, respectively. The strains of the shell are defined as follows (Rao, 2007)

$$\begin{aligned} &\varepsilon_x = \varepsilon_x^0 + zk_x \qquad \varepsilon_\theta = \varepsilon_\theta^0 + zk_\theta \qquad \varepsilon_{x\theta} = \varepsilon_{x\theta}^0 + zk_{x\theta} \\ &\varepsilon_{xz} = \varepsilon_{xz}^0 \qquad \varepsilon_{\theta z} = \varepsilon_{\theta z}^0 \end{aligned} \tag{2.2}$$

where (Rao, 2007)

$$\begin{aligned}
&\varepsilon_x^0 = \frac{\partial u_0}{\partial x} \qquad \varepsilon_\theta^0 = \frac{1}{R(x)}\frac{\partial v_0}{\partial \theta} + \frac{u_0 \sin\alpha}{R(x)} + \frac{w_0 \cos\alpha}{R(x)} \\
&\varepsilon_{x\theta}^0 = \frac{\partial v_0}{\partial x} + \frac{1}{R(x)}\frac{\partial u_0}{\partial \theta} - \frac{v_0 \sin\alpha}{R(x)} \qquad \varepsilon_{xz}^0 = \frac{\partial w_0}{\partial x} + \psi_x \\
&\varepsilon_{\theta z}^0 = \frac{1}{R(x)}\frac{\partial w_0}{\partial \theta} - \frac{v_0 \cos\alpha}{R(x)} + \psi_\theta \qquad k_x = \frac{\partial \psi_x}{\partial x} \\
&k_\theta = \frac{1}{R(x)}\Big(\frac{\partial \psi_\theta}{\partial \theta} + \psi_x \sin\alpha\Big) \qquad k_{x\theta} = \frac{\partial \psi_\theta}{\partial x} + \frac{1}{R(x)}\frac{\partial \psi_x}{\partial \theta} - \frac{\psi_\theta \sin\alpha}{R(x)}
\end{aligned} \tag{2.3}$$

The radius of the conical shell in any arbitrary point of its mid-surface is related to its position along x coordinate as

$$R(x) = R_1 + x \sin\alpha \tag{2.4}$$

The stress-strain relations of the k-th layer which is made of simple isotropic or magnetostrictive materials are defined as (Lee and Reddy, 2004)

$$\begin{Bmatrix} \sigma_x \\ \sigma_\theta \\ \sigma_{\theta z} \\ \sigma_{xz} \\ \sigma_{x\theta} \end{Bmatrix}^{(k)} = \begin{bmatrix} Q_{11} & Q_{12} & 0 & 0 & 0 \\ Q_{21} & Q_{22} & 0 & 0 & 0 \\ 0 & 0 & Q_{44} & 0 & 0 \\ 0 & 0 & 0 & Q_{55} & 0 \\ 0 & 0 & 0 & 0 & Q_{66} \end{bmatrix}^{(k)} \begin{Bmatrix} \varepsilon_x \\ \varepsilon_\theta \\ \varepsilon_{\theta z} \\ \varepsilon_{xz} \\ \varepsilon_{x\theta} \end{Bmatrix} - \begin{Bmatrix} e_{31} \\ e_{32} \\ 0 \\ 0 \\ 0 \end{Bmatrix}^{(k)} H \tag{2.5}$$

In the following, the superscript k which denotes the layers number is omitted for abbreviation. The plane stress reduced stiffnesses are obtained in the following form (Reddy, 2004)

$$\begin{aligned}
&Q_{11} = \frac{E}{1-\nu^2} \qquad Q_{12} = Q_{21} = \frac{\nu E}{1-\nu^2} \qquad Q_{22} = \frac{E}{1-\nu^2} \\
&Q_{66} = G \qquad Q_{44} = G \qquad Q_{55} = G
\end{aligned} \tag{2.6}$$

The variables E, G and ν are Young's moduli, shear moduli and Poisson's ratio, respectively. It should be mentioned that the values of e_{31} and e_{32} are zero for an isotropic material which is not magnetostrictive. The in-plane force resultants, N_x, N_θ and $N_{x\theta}$, the moment resultants, M_x, M_θ and $M_{x\theta}$ and transverse force resultants, Q_x, Q_θ are demonstrated in the following form (Pradhan and Reddy, 2004)

$$\begin{aligned}
&\begin{Bmatrix} N_x \\ N_\theta \\ M_x \\ M_\theta \end{Bmatrix} = \begin{bmatrix} A_{11} & A_{12} & B_{11} & B_{12} \\ A_{21} & A_{22} & B_{21} & B_{22} \\ B_{11} & B_{12} & D_{11} & D_{12} \\ B_{21} & B_{22} & D_{21} & D_{22} \end{bmatrix} \begin{Bmatrix} \varepsilon_x^0 \\ \varepsilon_\theta^0 \\ k_x \\ k_\theta \end{Bmatrix} - \begin{Bmatrix} A_{31} \\ A_{32} \\ B_{31} \\ B_{32} \end{Bmatrix} H \\
&\begin{Bmatrix} N_{x\theta} \\ M_{x\theta} \end{Bmatrix} = \begin{bmatrix} A_{66} & B_{66} \\ B_{66} & D_{66} \end{bmatrix} \begin{Bmatrix} \varepsilon_{x\theta}^0 \\ k_{x\theta} \end{Bmatrix} \qquad \begin{Bmatrix} Q_\theta \\ Q_x \end{Bmatrix} = K_s \begin{bmatrix} A_{44} & 0 \\ 0 & A_{55} \end{bmatrix} \begin{Bmatrix} \varepsilon_{\theta z}^0 \\ \varepsilon_{xz}^0 \end{Bmatrix}
\end{aligned} \tag{2.7}$$

where $K_s = 5/6$ (Reddy, 2004) and A_{ij}, B_{ij}, D_{ij} which are the laminate stiffness coefficients are obtained in the following form (Reddy, 2004)

$$\begin{aligned}
&A_{ij} = \sum_{k=1}^{N} Q_{ij}^{(k)}(z_{k+1} - z_k) \quad (i,j = 1,2) \qquad B_{ij} = \frac{1}{2}\sum_{k=1}^{N} Q_{ij}^{(k)}(z_{k+1}^2 - z_k^2) \quad (i,j = 1,2) \\
&D_{ij} = \frac{1}{3}\sum_{k=1}^{N} Q_{ij}^{(k)}(z_{k+1}^3 - z_k^3) \quad (i,j = 1,2) \qquad A_{ii} = \sum_{k=1}^{N} Q_{ii}^{(k)}(z_{k+1} - z_k) \quad (i = 4,5)
\end{aligned} \tag{2.8}$$

In Eq. (2.5), H is referred to the intensity of magnetic field of the magnetostrictive layers. The magnetic field is generated due to coil current I in the following form (Pradhan and Reddy, 2004;, Lee and Reddy, 2004)

$$H = k_c I \qquad k_c = \frac{n_c}{\sqrt{b_c^2 + 4r_c^2}} \tag{2.9}$$

where k_c is the magnetic coil constant which is related to coil width b_c, coil radius r_c and the number of the coil turns n_c. In order to design the control law and actively control the system vibration, the current I can be produced in relation with the velocities ($\dot{u}_0$ and $\dot{w}_0$) in the following form

$$I = -C(t)(\dot{u}_0 + \dot{w}_0) + \frac{H_b}{k_c} \tag{2.10}$$

where $C(t)$ is a control designing parameter and is considered to be constant in this study. In addition, H_b is the magnetic field of the bias point. Bias point is selected to be the middle point of the linear region of the strain versus magnetic field curve (Chapra and Sirohi, 2013). It should be mentioned that the second section of equation (2.10) (H_b/k_c) is static and does not come in vibration equations. The control gain value ckc is obtained in the following form

$$ckc = k_c C(t) \tag{2.11}$$

It should be mentioned that in Eq. (2.7), the magnetostrictive stiffness resultants, A_{31}, A_{32}, B_{31} and B_{32} are obtained as (Pradhan and Reddy, 2004)

$$[A_{31}, A_{32}, B_{31}, B_{32}] = \sum_{k=m_1,m_2,\ldots}^{N} \int_{z_k}^{z_{k+1}} ckc[e_{31}, e_{32}, ze_{31}, ze_{32}]\, dz \tag{2.12}$$

3. Problem solution

3.1. Basic relations

In this paper, Hamilton's principle is used to obtain vibration equations. Besides, in order to show the reliability of all results, two method including the Ritz and modified Galerkin methods are used for solving the problem. Hamilton's principle for free vibration is defined as follows (Rao, 2007)

$$\int_t (\delta T - \delta U_\varepsilon)\, dt = 0 \tag{3.1}$$

while δT and δU_ε are the virtual kinetic and strain energies which are calculated in the following form (Rao, 2007)

$$\begin{aligned}
\delta U_\varepsilon &= \int_x \int_\theta (N_x \delta\varepsilon_x^0 + N_\theta \delta\varepsilon_\theta^0 + N_{x\theta}\delta\varepsilon_{x\theta}^0 + M_x \delta k_x + M_\theta \delta k_\theta + M_{x\theta}\delta k_{x\theta} \\
&\quad + Q_x \delta\varepsilon_{xz}^0 + Q_\theta \delta\varepsilon_{\theta z}^0) R(x)\, d\theta\, dx \\
\delta T &= \int_\theta \int_x [J_1(\dot{u}_0\delta\dot{u}_0 + \dot{v}_0\delta\dot{v}_0 + \dot{w}_0\delta\dot{w}_0) + 2J_2(\dot{u}_0\delta\dot{\psi}_x + \delta\dot{u}_0\dot{\psi}_x + \dot{v}_0\delta\dot{\psi}_\theta + \delta\dot{v}_0\dot{\psi}_\theta) \\
&\quad + J_3(\dot{\psi}_x\delta\dot{\psi}_x + \dot{\psi}_\theta\delta\dot{\psi}_\theta)] R(x)\, dx\, d\theta
\end{aligned} \tag{3.2}$$

while J_1, J_2 and J_3 are mass moments of inertia which are calculated as (Qatu, 2004)

$$(J_1, J_2, J_3) = \sum_{k=1}^{N} \int_{z_k}^{z_{k+1}} \rho^{(k)}(1, z, z^2)\, dz \tag{3.3}$$

while ρ denotes the density of each layer. Hamilton's principle leads to differential vibration equations of the truncated conical shell via some simple mathematical operations

$$\begin{aligned}
&R(x)\frac{\partial N_x}{\partial x} + (N_x - N_\theta)\sin\alpha + \frac{\partial N_{x\theta}}{\partial \theta} - J_1 R(x)\ddot{u}_0 - J_2 R(x)\ddot{\psi}_x = 0\\
&Q_\theta \cos\alpha + R(x)\frac{\partial N_{x\theta}}{\partial x} + 2N_{x\theta}\sin\alpha + \frac{\partial N_\theta}{\partial \theta} - J_1\ddot{v}_0 R(x) - J_2\ddot{\psi}_\theta R(x) = 0\\
&-N_\theta \cos\alpha + \frac{\partial Q_x}{\partial x}R(x) + Q_x \sin\alpha + \frac{\partial Q_\theta}{\partial \theta} - J_1\ddot{w}_0 R(x) = 0\\
&R(x)\frac{\partial M_x}{\partial x} + (M_x - M_\theta)\sin\alpha + \frac{\partial M_{x\theta}}{\partial \theta} - Q_x R(x) - J_2 R(x)\ddot{u}_0 - J_3 R(x)\ddot{\psi}_x = 0\\
&R(x)\frac{\partial M_{x\theta}}{\partial x} + 2\sin\alpha M_{x\theta} + \frac{\partial M_\theta}{\partial \theta} - Q_\theta R(x) - J_2 R(x)\ddot{v}_0 - J_3 R(x)\ddot{\psi}_\theta = 0
\end{aligned} \tag{3.4}$$

In addition, the geometrical and natural boundary conditions are extracted from simplification of the Hamilton principle. The geometric and natural boundary conditions are respectively introduced in Eqs. (3.5) and (3.6) (Rao, 2007)

$$\begin{aligned}
&v_0(0,\theta,t) = 0 \qquad w_0(0,\theta,t) = 0 \qquad \psi_\theta(0,\theta,t) = 0\\
&v_0(L,\theta,t) = 0 \qquad w_0(L,\theta,t) = 0 \qquad \psi_\theta(L,\theta,t) = 0
\end{aligned} \tag{3.5}$$

$$\mathbf{NB}(0,\theta,t) = 0 \qquad \mathbf{NB}(L,\theta,t) = 0 \qquad \mathbf{NB} = \begin{Bmatrix} -N_x R(x) \\ 0 \\ 0 \\ -M_x R(x) \\ 0 \end{Bmatrix} \tag{3.6}$$

The following form of displacements and rotations could satisfy the geometrical boundary conditions of the system

$$\begin{Bmatrix} u_0 \\ v_0 \\ w_0 \\ \psi_x \\ \psi_\theta \end{Bmatrix} = \boldsymbol{\varphi}\mathbf{x}_t(t) \qquad \boldsymbol{\varphi} = \begin{Bmatrix} \sum\limits_{m=1}^{M}\sum\limits_{n=0}^{N_T} \cos\Big(\dfrac{m\pi x}{L}\Big)\cos(n\theta) \\ \sum\limits_{m=1}^{M}\sum\limits_{n=0}^{N_T} \sin\Big(\dfrac{m\pi x}{L}\Big)\sin(n\theta) \\ \sum\limits_{m=1}^{M}\sum\limits_{n=0}^{N_T} \sin\Big(\dfrac{m\pi x}{L}\Big)\cos(n\theta) \\ \sum\limits_{m=1}^{M}\sum\limits_{n=0}^{N_T} \cos\Big(\dfrac{m\pi x}{L}\Big)\cos(n\theta) \\ \sum\limits_{m=1}^{M}\sum\limits_{n=0}^{N_T} \sin\Big(\dfrac{m\pi x}{L}\Big)\sin(n\theta) \end{Bmatrix} \tag{3.7}$$

$$\mathbf{x}_t(t) = [\mathbf{u}_{t_{mn}}(t), \mathbf{v}_{t_{mn}}(t), \mathbf{w}_{t_{mn}}(t), \boldsymbol{\psi}_{xt_{mn}}(t), \boldsymbol{\psi}_{\theta t_{mn}}(t)]$$

while m and n express longitudinal and circumferential wave numbers, respectively. Besides, the bounding values of m and n are considered to be M and N_T, respectively. The effects of bounding values of wave numbers on the convergence of frequency factor responses are investigated in Section 4.

3.2. Ritz method

The Ritz method (Reddy, 2002, 2004) employes variational statements. The variational form of strain and kinetic energies for free vibration can be obtained from Eqs. (3.2) in the following form

$$\begin{aligned}
\delta U_\varepsilon &= \int_x \int_\theta \Big[N_x \frac{\partial \delta u_0}{\partial x} + \frac{N_\theta}{R(x)} \Big(\frac{\partial \delta v_0}{\partial \theta} + \delta u_0 \sin\alpha + \delta w_0 \cos\alpha \Big) \\
&+ N_{x\theta} \Big(\frac{\partial \delta v_0}{\partial x} + \frac{1}{R(x)} \frac{\partial \delta u_0}{\partial \theta} - \frac{\delta v_0 \sin\alpha}{R(x)} \Big) + M_x \frac{\partial \delta \psi_x}{\partial x} + \frac{M_\theta}{R(x)} \Big(\frac{\partial \delta \psi_\theta}{\partial \theta} + \delta \psi_x \sin\alpha \Big) \\
&+ M_{x\theta} \Big(\frac{\partial \delta \psi_\theta}{\partial x} + \frac{1}{R(x)} \frac{\partial \delta \psi_x}{\partial \theta} - \frac{\delta \psi_\theta \sin\alpha}{R(x)} \Big) + Q_x \Big(\frac{\partial \delta w_0}{\partial x} + \delta \psi_x \Big) \\
&+ Q_\theta \Big(\frac{1}{R(x)} \frac{\partial \delta w_0}{\partial \theta} - \frac{\delta v_0 \cos\alpha}{R(x)} + \delta \psi_\theta \Big) \Big] R(x)\, dx\, d\theta \\
\delta T &= J_1 \int_\theta \int_x (\dot{u}_0 \delta \dot{u}_0 + \dot{v}_0 \delta \dot{v}_0 + \dot{w}_0 \delta \dot{w}_0) R(x)\, dx\, d\theta \\
&+ J_2 \int_\theta \int_x (\dot{\psi}_x \delta \dot{u}_0 + \dot{u}_0 \delta \dot{\psi}_x + \dot{\psi}_\theta \delta \dot{v}_0 + \dot{v}_0 \delta \dot{\psi}_\theta) R(x)\, dx\, d\theta \\
&+ J_3 \int_x \int_z (\dot{\psi}_x \delta \dot{\psi}_x + \dot{\psi}_\theta \delta \dot{\psi}_\theta) R(x)\, dz\, dx
\end{aligned} \tag{3.8}$$

Substitution of Eqs. (2.2), (2.3), (2.7), (2.9), (2.10) and (2.11) into Eqs. (3.8) and then substitution of the obtained result into Eq. (3.1) leads to the following equation

$$\int_t \int_x \int_\theta \begin{bmatrix} S_{11} & S_{12} & S_{13} & S_{14} & S_{15} \\ S_{21} & S_{22} & S_{23} & S_{24} & S_{25} \\ S_{31} & S_{32} & S_{33} & S_{34} & S_{35} \\ S_{41} & S_{42} & S_{43} & S_{44} & S_{45} \\ S_{51} & S_{52} & S_{53} & S_{54} & S_{55} \end{bmatrix} \begin{Bmatrix} u_0 \\ v_0 \\ w_0 \\ \psi_x \\ \psi_\theta \end{Bmatrix} = 0 \tag{3.9}$$

while S_{ij} are differential operators defined as follows

$$\begin{aligned}
S_{11} &= A_{11} R(x) \frac{\partial U_p}{\partial x} \frac{\partial}{\partial x} + A_{12} \frac{\partial U_p}{\partial x} \sin\alpha + A_{12} U_p \sin\alpha \frac{\partial}{\partial x} + \frac{A_{22} U_p \sin^2\alpha}{R(x)} + \frac{A_{66}}{R(x)} \frac{\partial U_p}{\partial \theta} \frac{\partial}{\partial \theta} \\
&+ J_1 U_p R(x) \frac{\partial^2}{\partial t^2} - ckc \Big(A_{31} \frac{\partial U_p}{\partial x} R(x) + A_{32} U_p \sin\alpha \Big) \frac{\partial}{\partial t} \\
S_{12} &= A_{12} \frac{\partial U_p}{\partial x} \frac{\partial}{\partial \theta} + \frac{A_{22} U_p \sin\alpha}{R(x)} \frac{\partial}{\partial \theta} - A_{66} \frac{\partial U_p}{\partial \theta} \frac{\sin\alpha}{R(x)} + A_{66} \frac{\partial U_p}{\partial \theta} \frac{\partial}{\partial x} \\
S_{13} &= A_{12} \frac{\partial U_p}{\partial x} \cos\alpha + \frac{A_{22} U_p \sin\alpha \cos\alpha}{R(x)} - ckc \Big(A_{31} R(x) \frac{\partial U_p}{\partial x} + A_{32} U_p \sin\alpha \Big) \frac{\partial}{\partial t} \\
S_{14} &= J_2 U_p R(x) \frac{\partial^2}{\partial t^2} \qquad S_{15} = 0 \\
S_{21} &= A_{12} \frac{\partial V_p}{\partial \theta} \frac{\partial}{\partial x} + A_{22} \frac{\partial V_p}{\partial \theta} \frac{\sin\alpha}{R(x)} + A_{66} \frac{\partial V_p}{\partial x} \frac{\partial}{\partial \theta} - \frac{A_{66} V_p \sin\alpha}{R(x)} \frac{\partial}{\partial \theta} - ckc A_{32} \frac{\partial V_p}{\partial \theta} \frac{\partial}{\partial t} \\
S_{22} &= \frac{A_{22}}{R(x)} \frac{\partial V_p}{\partial \theta} \frac{\partial}{\partial \theta} - A_{66} \frac{\partial V_p}{\partial x} \sin\alpha + A_{66} \frac{\partial V_p}{\partial x} R(x) \frac{\partial}{\partial x} + \frac{A_{66} V_p \sin^2\alpha}{R(x)} - A_{66} V_p \sin\alpha \frac{\partial}{\partial x} \\
&+ \frac{K_s V_p A_{44} \cos^2\alpha}{R(x)} + J_1 V_p R(x) \frac{\partial^2}{\partial t^2}
\end{aligned}$$

$$S_{23}=\frac{A_{22}\cos\alpha}{R(x)}\frac{\partial V_p}{\partial\theta}-\frac{K_sA_{44}V_p\cos\alpha}{R(x)}\frac{\partial}{\partial\theta}-ckcA_{32}\frac{\partial V_p}{\partial\theta}\frac{\partial}{\partial t}\qquad S_{24}=0$$

$$S_{25}=-K_sA_{44}V_p\cos\alpha+J_2V_pR(x)\frac{\partial^2}{\partial t^2}$$

$$S_{31}=A_{12}W_p\cos\alpha\frac{\partial}{\partial x}+\frac{A_{22}W_p\sin\alpha\cos\alpha}{R(x)}-ckcA_{32}W_p\cos\alpha\frac{\partial}{\partial t}$$

$$S_{32}=\frac{A_{22}W_p\cos\alpha}{R(x)}\frac{\partial}{\partial\theta}-\frac{K_sA_{44}\cos\alpha}{R(x)}\frac{\partial W_p}{\partial\theta}$$

$$S_{33}=\frac{A_{22}W_p\cos^2\alpha}{R(x)}+K_sA_{55}R(x)\frac{\partial W_p}{\partial x}\frac{\partial}{\partial x}+\frac{K_sA_{44}}{R(x)}\frac{\partial W_p}{\partial\theta}\frac{\partial}{\partial\theta}+J_1W_pR(x)\frac{\partial^2}{\partial t^2}$$
$$-ckc\Big(A_{32}W_p\cos\alpha\frac{\partial}{\partial t}\Big)$$

$$S_{34}=K_sA_{55}\frac{\partial W_p}{\partial x}R(x)\qquad S_{35}=K_sA_{44}\frac{\partial W_p}{\partial\theta}$$

$$S_{41}=J_2R(x)\psi_{xp}\frac{\partial^2}{\partial t^2}\qquad S_{42}=0\qquad S_{43}=K_sA_{55}\psi_{xp}R(x)\frac{\partial}{\partial x}$$

$$S_{44}=D_{11}R(x)\frac{\partial\psi_{xp}}{\partial x}\frac{\partial}{\partial x}+D_{12}\frac{\partial\psi_{xp}}{\partial x}\sin\alpha+D_{12}\psi_{xp}\sin\alpha\frac{\partial}{\partial x}+\frac{D_{22}\psi_{xp}\sin^2\alpha}{R(x)}$$
$$+\frac{D_{66}}{R(x)}\frac{\partial\psi_{xp}}{\partial\theta}\frac{\partial}{\partial\theta}+K_sA_{55}\psi_{xp}R(x)+J_3\psi_{xp}R(x)\frac{\partial^2}{\partial t^2}$$

$$S_{45}=D_{12}\frac{\partial\psi_{xp}}{\partial\theta}\frac{\partial}{\partial\theta}+\frac{D_{22}\psi_{xp}\sin\alpha}{R(x)}\frac{\partial}{\partial\theta}+D_{66}\frac{\partial\psi_{xp}}{\partial\theta}\frac{\partial}{\partial x}-\frac{D_{66}\sin\alpha}{R(x)}\frac{\partial\psi_{xp}}{\partial\theta}$$

$$S_{51}=0\qquad S_{52}=-K_sA_{44}\psi_{\theta p}\cos\alpha+J_2\psi_{\theta p}R(x)\frac{\partial^2}{\partial t^2}\qquad S_{53}=K_sA_{44}\psi_{\theta p}\frac{\partial}{\partial\theta}$$

$$S_{54}=D_{12}\frac{\partial\psi_{\theta p}}{\partial\theta}\frac{\partial}{\partial x}+\frac{D_{22}\sin\alpha}{R(x)}\frac{\partial\psi_{\theta p}}{\partial\theta}+D_{66}\frac{\partial\psi_{\theta p}}{\partial x}\frac{\partial}{\partial\theta}-\frac{D_{66}\psi_{\theta p}\sin\alpha}{R(x)}\frac{\partial}{\partial\theta}$$

$$S_{55}=\frac{D_{22}}{R(x)}\frac{\partial\psi_{\theta p}}{\partial\theta}\frac{\partial}{\partial\theta}+D_{66}R(x)\frac{\partial\psi_{\theta p}}{\partial x}\frac{\partial}{\partial x}-D_{66}\frac{\partial\psi_{\theta p}}{\partial x}\sin\alpha-D_{66}\psi_{\theta p}\sin\alpha\frac{\partial}{\partial x}$$
$$+\frac{D_{66}\psi_{\theta p}\sin^2\alpha}{R(x)}+K_sA_{44}\psi_{\theta p}R(x)+J_3R(x)\psi_{\theta p}\frac{\partial^2}{\partial t^2}$$

while U_p, V_p, W_p, ψ_{xp} and $\psi_{\theta p}$ are referred to the parts of virtual displacements which are dependent to $\mathbf{x}$ and θ. The approximate function of this method is only necessary to satisfy geometrical boundary conditions (Reddy, 2002, 2004). Therefore, substitution of Eq. (3.7) which satisfies geometric boundary conditions into Eq. (3.9) leads to the following ordinary differential equation

$$\mathbf{M}\ddot{\mathbf{x}}_t(t)+\mathbf{C}\dot{\mathbf{x}}_t(t)+\mathbf{K}\mathbf{x}_t(t)=\mathbf{0} \tag{3.10}$$

3.3. Modified Galerkin method

The Galerkin method is (Rao, 2007) from weighted residual methods with trial solution which is necessary to satisfy all of the boundary conditions. Differential equations of the system which introduced in Eqs. (3.4) can be rewritten in the following form

$$\mathbf{L}\begin{Bmatrix}u_0\\v_0\\w_0\\\psi_x\\\psi_\theta\end{Bmatrix}=\begin{bmatrix}L_{11}&L_{12}&L_{13}&L_{14}&L_{15}\\L_{21}&L_{22}&L_{23}&L_{24}&L_{25}\\L_{31}&L_{32}&L_{33}&L_{34}&L_{35}\\L_{41}&L_{42}&L_{43}&L_{44}&L_{45}\\L_{51}&L_{52}&L_{53}&L_{54}&L_{55}\end{bmatrix}\begin{Bmatrix}u_0\\v_0\\w_0\\\psi_x\\\psi_\theta\end{Bmatrix}=\mathbf{0} \tag{3.11}$$

The coefficients L_{ij} which denote differential operators $\mathbf{L}$ of vibration equations are defined in the following

$$L_{11} = A_{11}R(x)\frac{\partial^2}{\partial x^2} - \frac{A_{22}\sin^2\alpha}{R(x)} + \frac{A_{66}}{R(x)}\frac{\partial^2}{\partial\theta^2} + A_{11}\sin\alpha\frac{\partial}{\partial x} + ckc\Big(-A_{31}R(x)\frac{\partial^2}{\partial x\partial t} - A_{31}\sin\alpha\frac{\partial}{\partial t} + A_{32}\sin\alpha\frac{\partial}{\partial t}\Big) - R(x)J_1\frac{\partial^2}{\partial t^2}$$

$$L_{12} = A_{12}\frac{\partial^2}{\partial x\partial\theta} - \frac{A_{22}\sin\alpha}{R(x)}\frac{\partial}{\partial\theta} + A_{66}\frac{\partial^2}{\partial x\partial\theta} - \frac{A_{66}x\sin^2\alpha}{R(x)^2}\frac{\partial}{\partial\theta} - \frac{A_{66}R_1}{R(x)^2}\frac{\partial}{\partial\theta}$$

$$L_{13} = A_{12}\cos\alpha\frac{\partial}{\partial x} - \frac{A_{22}\cos\alpha\sin\alpha}{R(x)} + ckc\Big(-A_{31}R(x)\frac{\partial^2}{\partial x\partial t} - A_{31}\sin\alpha\frac{\partial}{\partial t} + A_{32}\sin\alpha\frac{\partial}{\partial t}\Big)$$

$$L_{14} = -J_2R(x) \qquad L_{15} = 0$$

$$L_{21} = A_{12}\frac{\partial^2}{\partial x\partial\theta} + \frac{A_{22}\sin\alpha}{R(x)}\frac{\partial}{\partial\theta} + \frac{A_{66}\sin\alpha}{R(x)}\frac{\partial}{\partial\theta} + A_{66}\frac{\partial^2}{\partial x\partial\theta} - A_{32}ckc\frac{\partial^2}{\partial\theta\partial t}$$

$$L_{22} = \frac{A_{22}}{R(x)}\frac{\partial^2}{\partial\theta^2} - \frac{A_{66}\sin^2\alpha}{R(x)} + A_{66}R(x)\frac{\partial^2}{\partial x^2} + A_{66}\sin\alpha\frac{\partial}{\partial x} - \frac{K_sA_{44}\cos^2\alpha}{R(x)} - J_1R(x)\frac{\partial^2}{\partial t^2}$$

$$L_{23} = \frac{K_sA_{44}\cos\alpha}{R(x)}\frac{\partial}{\partial\theta} + \frac{A_{22}\cos\alpha}{R(x)}\frac{\partial}{\partial\theta} - A_{32}ckc\frac{\partial^2}{\partial\theta\partial t}$$

$$L_{24} = 0 \qquad L_{25} = K_sA_{44}\cos\alpha - R(x)J_2\frac{\partial^2}{\partial t^2}$$

$$L_{31} = -A_{12}\cos\alpha\frac{\partial}{\partial x} - \frac{A_{22}\cos\alpha\sin\alpha}{R(x)} + ckc\Big(A_{32}\cos\alpha\frac{\partial}{\partial t}\Big)$$

$$L_{32} = -\frac{A_{22}\cos\alpha}{R(x)}\frac{\partial}{\partial\theta} - \frac{K_sA_{44}\cos\alpha}{R(x)}\frac{\partial}{\partial\theta}$$

$$L_{33} = -\frac{A_{22}\cos^2\alpha}{R(x)} + K_sA_{55}\sin\alpha\frac{\partial}{\partial x} + K_sA_{55}R(x)\frac{\partial^2}{\partial x^2} + \frac{K_sA_{44}}{R(x)}\frac{\partial^2}{\partial\theta^2} + ckc\Big(A_{32}\cos\alpha\frac{\partial}{\partial t}\Big) - R(x)J_1\frac{\partial^2}{\partial t^2}$$

$$L_{34} = K_sA_{55}R(x)\frac{\partial}{\partial x} + K_sA_{55}\sin\alpha \qquad L_{35} = K_sA_{44}\frac{\partial}{\partial\theta}$$

$$L_{41} = -R(x)J_2\frac{\partial^2}{\partial t^2} \qquad L_{42} = 0 \qquad L_{43} = -R_1K_sA_{55}\frac{\partial}{\partial x} - x\sin\alpha K_sA_{55}\frac{\partial}{\partial x}$$

$$L_{44} = D_{11}R(x)\frac{\partial^2}{\partial x^2} + D_{11}\sin\alpha\frac{\partial}{\partial x} - \frac{D_{22}\sin^2\alpha}{R(x)} + \frac{D_{66}}{R(x)}\frac{\partial^2}{\partial\theta^2} - R(x)K_sA_{55} - J_3R(x)\frac{\partial^2}{\partial t^2}$$

$$L_{45} = D_{12}\frac{\partial^2}{\partial x\partial\theta} - \frac{D_{22}\sin\alpha}{R(x)}\frac{\partial}{\partial\theta} + D_{66}\frac{\partial^2}{\partial x\partial\theta} - \frac{D_{66}\sin\alpha}{R(x)}\frac{\partial}{\partial\theta}$$

$$L_{51} = 0 \qquad L_{52} = K_sA_{44}\cos\alpha - J_2R(x)\frac{\partial^2}{\partial t^2} \qquad L_{53} = -K_sA_{44}\frac{\partial}{\partial\theta}$$

$$L_{54} = D_{12}\frac{\partial^2}{\partial x\partial\theta} + \frac{D_{22}\sin\alpha}{R(x)}\frac{\partial}{\partial\theta} + D_{66}\frac{\partial^2}{\partial x\partial\theta} + \frac{D_{66}\sin\alpha}{R(x)}\frac{\partial}{\partial\theta}$$

$$L_{55} = \frac{D_{22}}{R(x)}\frac{\partial^2}{\partial\theta^2} + D_{66}R(x)\frac{\partial^2}{\partial x^2} + D_{66}\sin\alpha\frac{\partial}{\partial x} - \frac{D_{66}}{R(x)}\sin^2\alpha - K_sA_{44}R(x) - J_3R(x)\frac{\partial^2}{\partial t^2}$$

In addition, natural boundary conditions which introduced in equation (3.6) can be rewritten in the following form

$$\mathbf{P}\begin{Bmatrix} u_0(0,\theta,t) \\ v_0(0,\theta,t) \\ w_0(0,\theta,t) \\ \psi_x(0,\theta,t) \\ \psi_\theta(0,\theta,t) \end{Bmatrix} = \mathbf{0} \qquad \mathbf{P}\begin{Bmatrix} u_0(L,\theta,t) \\ v_0(L,\theta,t) \\ w_0(L,\theta,t) \\ \psi_x(L,\theta,t) \\ \psi_\theta(L,\theta,t) \end{Bmatrix} = \mathbf{0}$$

$$\mathbf{P} = \begin{bmatrix} P_{11} & P_{12} & P_{13} & 0 & 0 \\ 0 & 0 & 0 & 0 & 0 \\ 0 & 0 & 0 & 0 & 0 \\ 0 & 0 & 0 & P_{44} & P_{45} \\ 0 & 0 & 0 & 0 & 0 \end{bmatrix} \tag{3.12}$$

$$P_{11} = -A_{11}R(x)\frac{\partial}{\partial x} - A_{12}\sin\alpha + A_{31}R(x)\frac{\partial}{\partial t} \qquad P_{12} = -A_{12}\frac{\partial}{\partial\theta}$$

$$P_{13} = -A_{12}\cos\alpha + A_{31}R(x)\frac{\partial}{\partial t}$$

$$P_{44} = -D_{11}R(x)\frac{\partial}{\partial x} - D_{12}\sin\alpha \qquad P_{45} = -D_{12}\frac{\partial}{\partial\theta}$$

The modified Galerkin method formulation can be written as follows

$$\int_0^L \int_0^{2\pi} \Big(\mathbf{L}\boldsymbol{\varphi}\mathrm{e}^{\lambda t}\Big)\boldsymbol{\varphi}\, d\theta\, dx - \int_0^{2\pi} \Big(\mathbf{P}\boldsymbol{\varphi}\mathrm{e}^{\lambda t}\Big)\boldsymbol{\varphi}\Big|_0^L d\theta = \mathbf{0} \tag{3.13}$$

The Galerkin method trial function vector should satisfy both natural and geometrical boundary conditions (Rao, 2007). The shape vector $\boldsymbol{\varphi}$ which introduced in Eq. (3.7) only satisfies the geometrical boundary conditions. Therefore, the natural boundary conditions are added into the Galerkin method formulation in order to compensate its imperfection. Finally, an ordinary differential equation like Eq. (3.10) is extracted from Eq. (3.13).

3.4. Extraction of frequencies and displacement

In order to obtain the frequency and displacement of the shell, it is appropriate to write Eq. (3.10) in the state space form as follows

$$\dot{\mathbf{y}}(t) = \mathbf{A}\mathbf{y}(t) \tag{3.14}$$

while

$$\mathbf{y}(t) = [\mathbf{x}_t(t), \dot{\mathbf{x}}_t(t)]^{\mathrm{T}} \qquad \mathbf{A} = \begin{bmatrix} \mathbf{0} & \mathbf{I} \\ -\mathbf{M}^{-1}\mathbf{K} & -\mathbf{M}^{-1}\mathbf{C} \end{bmatrix} \tag{3.15}$$

The two smallest eigenvalues of the matrix $\mathbf{A}$ are the fundamental responses which are shown as: $\lambda = -\beta \pm \mathrm{i}\omega$. It should be mentioned that β and ω are respectively referred to damping coefficient and frequency. The time response of the shell vibration is obtained in the following form

$$\mathbf{y}(t) = \exp(\mathbf{A}t)\mathbf{y}_0 \tag{3.16}$$

while $\mathbf{y}_0$ is the initial time response of the shell. Substitution of Eq. (3.16) into Eq. (3.7) and then substitution of the result into Eq. (2.1) leads to the displacement of any point of the shell.

4. Results and discussions

In this Section, the results of active vibration control for an isotropic truncated conical shell embedded with two magnetostrictive layers is illustrated. It should be mentioned that in order to show the correctness of this study, all of the results of this Section obtained using the two Ritz and modified Galerkin methods. At first, the convergence and accuracy of the Ritz and modified Galerkin methods results are presented. In order to obtain the results of convergence and accuracy which are tabulated in Tables 1 to 3, the variable values are considered to be $L\sin\alpha/R_2 = 0.25$, $h/R_2 = 0.01$ and $\nu = 0.3$. The frequency factor which is a dimensionless parameter is defined in the following form (Irie *et al.*, 1984; Lam and Hua, 1999)

$$\gamma = \omega R_2\sqrt{\frac{\rho(1-\nu^2)}{E}} \tag{4.1}$$

Table 1 tabulates the effect of the longitudinal wave number bounding value M on the convergence of the frequency factor obtained for mode shape with $n = 9$ for a conical shell with $\alpha = 30^\circ$. The longitudinal wave number bounding value M varies from 1 to 5. As can be seen from Table 1, the convergence rate is great, and the convergence of the frequency factor is obtained only for $M = 2$. Table 2 illustrates the effect of N_T on the frequency factor for the mode shape with $n = 9$ for a conical shell with $\alpha = 30^\circ$. The variable N_T varies from 9 to 12 while M is considered to be 3. It is obvious from Table 2 that the increase of N_T never changes the value of the frequency factor. This result may arise from the symmetric geometry of the truncated conical shell.

Table 1. The effect of an increase in the longitudinal wave number M on the frequency factor

M ($N_T = 9$)	Present Ritz method	Present modified Galerkin method	Irie *et al.* (1984)	Lam and Hua (1999)
1	0.5634	0.5634	0.4892	0.4916
2	0.4884	0.4884		
3	0.4884	0.4884		
4	0.4879	0.4879		
5	0.4879	0.4879		

Table 2. The effect of an increase in the circumferential wave number N_T on the convergence of the frequency factor

N_T ($M = 3$)	Present Ritz method	Present modified Galerkin method	Irie *et al.* (1984)	Lam and Hua (1999)
9	0.4884	0.4884	0.4892	0.4916
10	0.4884	0.4884		
11	0.4884	0.4884		
12	0.4884	0.4884		

Now in the next step, the accuracy of the Ritz and modified Galerkin methods results is validated by comparing with literature results and also finite element software results for conical shells with $\alpha = 30^\circ$ and $\alpha = 45^\circ$. It should be mentioned that in obtaining the results of Table 3, the longitudinal wave number's bounding value is considered to be 3 and 2 for Ritz and modified Galerkin methods, respectively. It can be seen that there is good agreement between the results of Ritz and modified Galerkin methods, finite element software and literature.

In the next step, the effect of using magnetostrictive layers on active vibration control of the conical shells for the mode shape with $n = 3$ is investigated. An aluminum truncated conical shell

Table 3. Comparison of the results of the Ritz and modified Galerkin methods with finite element software and literature results

n	$\alpha = 30°$					$\alpha = 45°$				
	Ritz method	Modified Galerkin method	[12]	[17]	Finite element	Ritz method	Modified Galerkin method	[12]	[17]	Finite element
2	0.8316	0.8317	0.7910	0.8420	0.7954	0.7606	0.7606	0.6879	0.7655	0.7116
3	0.7331	0.7331	0.7284	0.7376	0.7220	0.7175	0.7175	0.6973	0.7212	0.7046
4	0.6340	0.6340	0.6352	0.6362	0.6288	0.6711	0.6711	0.6664	0.6739	0.6688
5	0.5513	0.5514	0.5531	0.5528	0.5477	0.6300	0.6300	0.6304	0.6323	0.6304
6	0.4937	0.4939	0.4949	0.4950	0.4902	0.6013	0.6014	0.6032	0.6035	0.6017
7	0.4647	0.4648	0.4653	0.4661	0.4605	0.5896	0.5897	0.5918	0.5921	0.5891
8	0.4639	0.4640	0.4645	0.4660	0.4590	0.5969	0.5970	0.5992	0.6001	0.5954
9	0.4884	0.4884	0.4892	0.4916	0.4824	0.6232	0.6233	0.6257	0.6273	0.6208

[12] – Irie *et al.* (1984), [17] – Lam and Hua (1999)

embedded with two magnetostrictive layers is considered here. The conical shell length, large edge radius and semi-vertex angle are respectively 0.9 m, 1 m and 45°. In addition, aluminum and magnetostrictive layers thicknesses are considered to be 1 mm and 3 mm, respectively. Besides, the initial speed, the bounding value of longitudinal wave number and control gain are assumed to be 0.5 m/s, 2 and 10^4, respectively. These mentioned values are used in the next part of the paper unless mentioned otherwise. The magnetostrictive material which is used here is Terfenol-D. The values of Terfenol-D characteristics are considered as (Pradhan and Reddy, 2004; Lee and Reddy, 2004): $E_m = 26.5G$ Pa, $d_m = 1.67 \cdot 10^{-8}$ m/A, $\nu_m = 0$, $\rho_m = 9250\,\mathrm{kg/m^3}$.

Figures 2a and 2b reveal the effect of using active vibration control on the displacement in the thickness direction versus time for a point on the shell with position $(x, \theta, z) = (0.5L, 0, 0)$ using the Ritz and modified Galerkin methods respectively. When the vibration control is not used ($ckc = 0$), the system vibration response is not damped. On the other hand, as the value of control gain ckc increases, faster vibration suppression takes place.

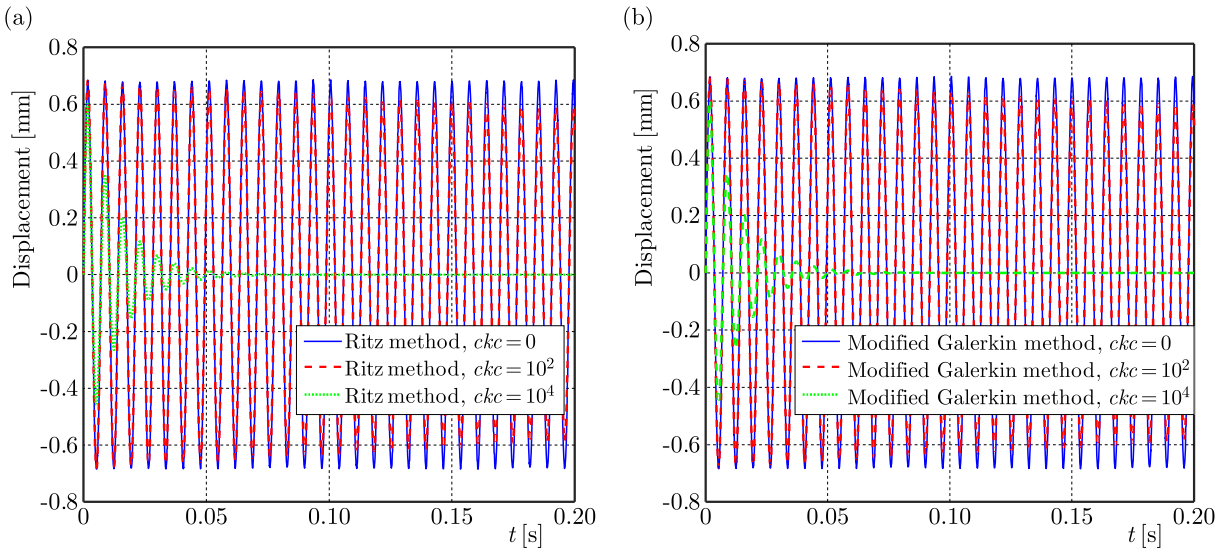

Fig. 2. The effect of the control gain value on the displacement of the shell in the thickness direction: (a) Ritz method, (b) modified Galerkin method

Figures 3a and 3b demonstrate, respectively, the effect of magnetostrictive layers thickness on the damping coefficient and frequency of the conical shell. Figure 3a shows that the damping

coefficient increases with the increase of magnetostrictive layers thickness, which leads to faster vibration suppression. Figure 3b reveals that as the value of magnetostrictive layers thickness increases, the value of frequency decreases.

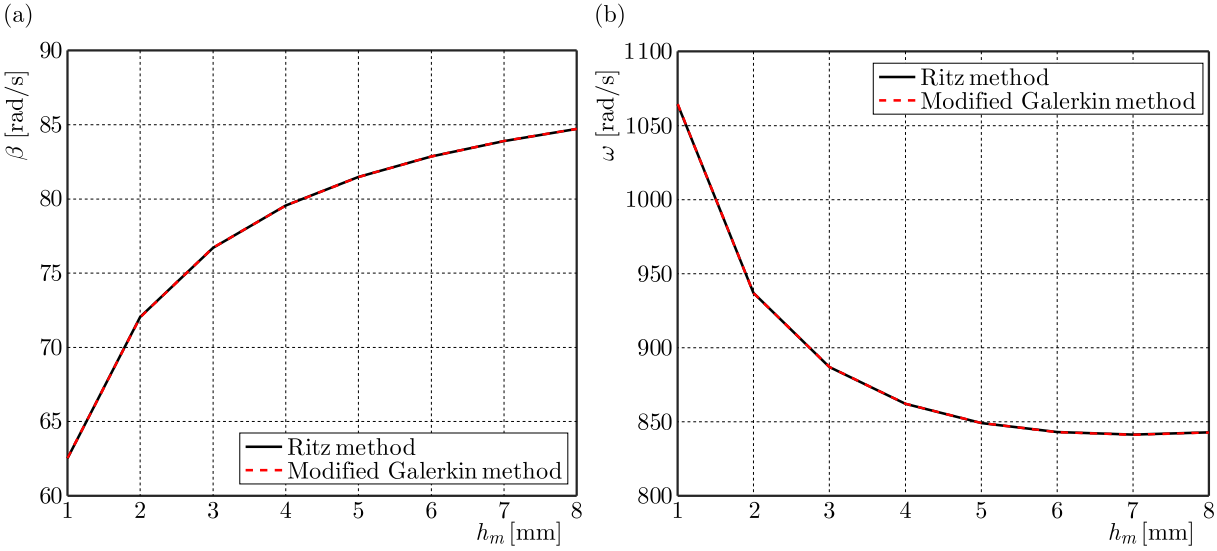

Fig. 3. The influence of magnetostrictive layers thickness on: (a) damping coefficient, (b) frequency

Figures 4a and 4b depict the effect of magnetostrictive layers thickness on the displacement of the shell in the thickness direction through the Ritz and modified Galerkin methods, respectively. It is obvious from Figs. 4a and 4b that vibration suppression takes place faster for the conical shells with greater values of the magnetostrictive layers thickness; therefore, Fig. 4 corroborates the results of Fig. 3.

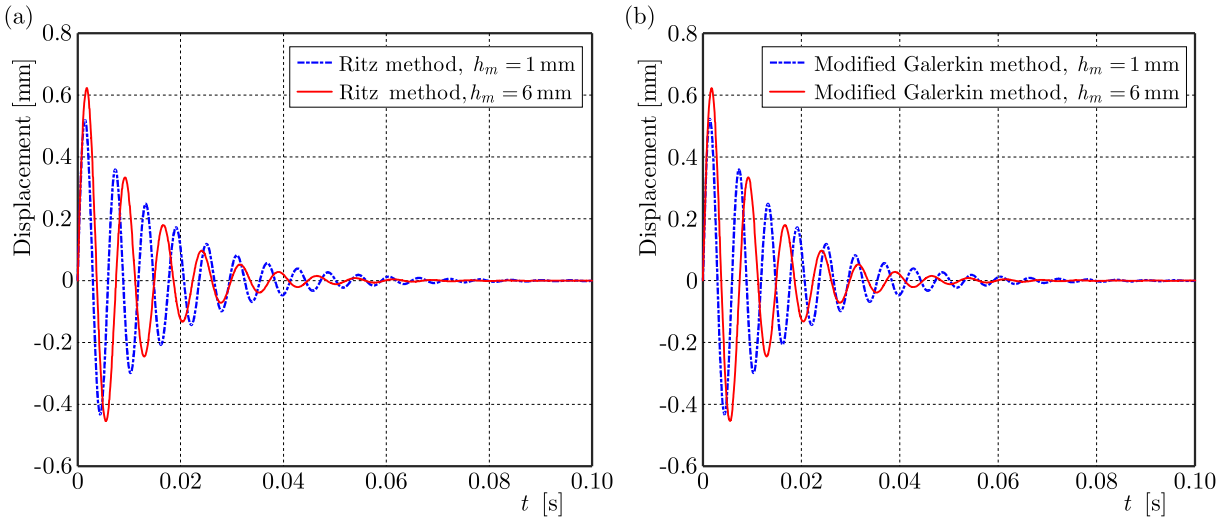

Fig. 4. Displacement of the truncated conical shell in the thickness direction for different values of magnetostrictive layers thickness: (a) Ritz method, (b) modified Galerkin method

Figures 5a and 5b show, respectively, damping coefficient and frequency diagrams versus isotropic layer thickness. One can conclude from Fig. 5a that the increase of isotropic layer thickness leads to a decrease in the damping coefficient, which leads to slower vibration suppression. It is obvious from Fig. 5b that as the thickness of isotropic layer increases, the value of frequency becomes greater.

Figure 6a demonstrates the diagram of the damping coefficient versus length of the conical shell. As the value of length increases, the damping coefficient gets smaller, which leads to slower

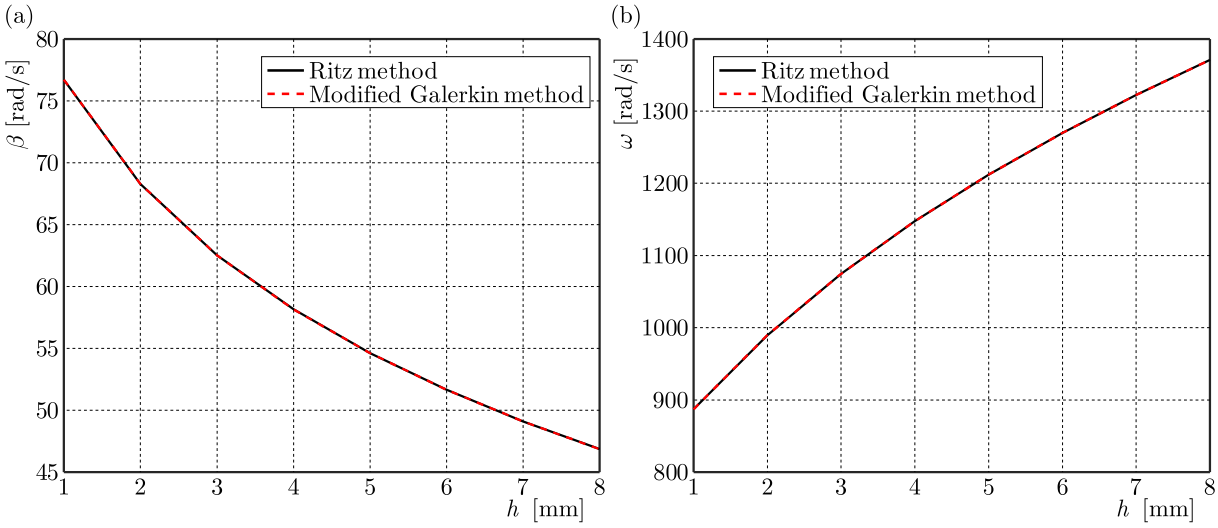

Fig. 5. The effect of isotropic layer thickness on the: (a) damping coefficient, (b) frequency

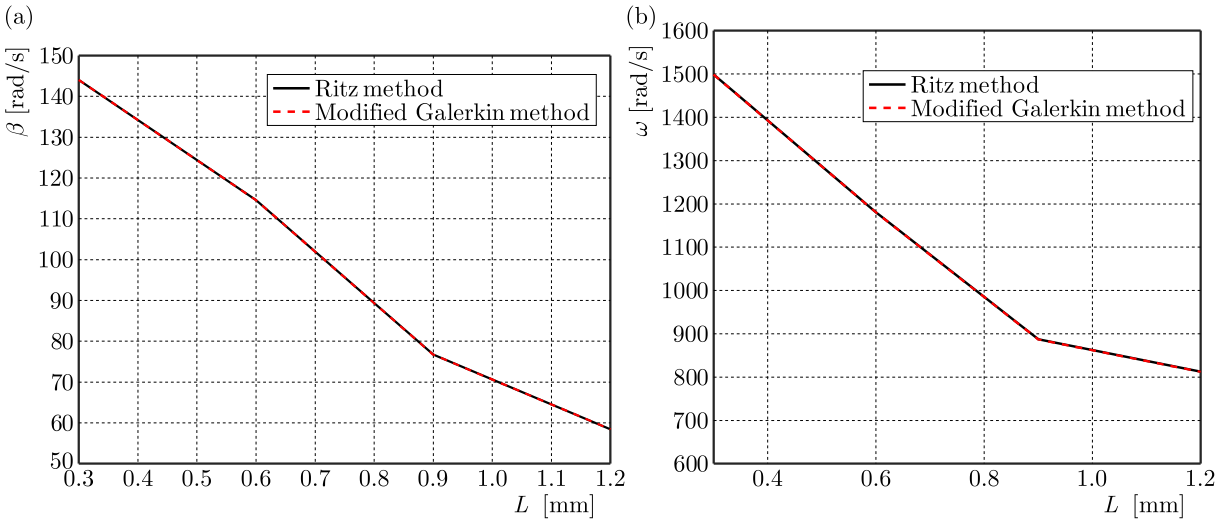

Fig. 6. The effect of length of the truncated conical shell on the: (a) damping coefficient, (b) frequency

vibration attenuation. Figure 6b shows the frequency of the conical shell versus length of the shell. This figure reveals that the conical shell with the largest length has the lowest frequency.

Table 4 shows the effect of semi-vertex angle on the vibration characteristics of the conical shell. For the results of Table 4, the bounding value of longitudinal wave number is considered to be 3 and 2 for Ritz and modified Galerkin methods, respectively. It is obvious from Table 4 that the increase of semi-vertex angle leads to smaller values of the damping coefficient. Therefore, vibration of the conical shell with the largest semi-vertex angle suppress with the slowest rate. In addition, the increase of semi-vertex angle leads to smaller values for the frequency.

Table 4. Variations of the damping coefficient and frequency with the semi-vertex angle of the conical shell

α	Ritz method		Modified Galerkin method	
	β [rad/s]	ω [rad/s]	β [rad/s]	ω [rad/s]
30°	93.8739	1005.3576	93.9962	1007.7142
45°	75.6201	871.9880	76.7118	887.0433
60°	54.6779	694.3874	57.3261	716.9652
75°	30.8688	413.2493	31.7141	441.3442

5. Conclusion

In this paper, active vibration control of an isotropic truncated conical shell embedded with magnetostrictive layers as actuators with simply supported boundary conditions on both sides is investigated. Velocity feedback control formulation is applied to extract a closed loop control law. The first order shear deformation theory and the Hamilton principle are used for extracting the vibration equations. The Ritz and modified Galerkin methods are used to convert the kinematic equations of the conical shell, which are partial differential equations, into ordinary differential equations. The accuracy and correctness of the results of this study are proved by comparing with the literature and finite element software results. The effects of several parameters including the control gain value, thickness of the magnetostrictive layers, isotropic layer thickness, length and semi-vertex angle of the truncated conical shell on the vibration suppression characteristics are illustrated in details. The results show that as the control gain value or thickness of the magnetostrictive layers increases, the system vibration response attenuates quicker. On the other hand, the rate of vibration suppression decreases with the increase of the isotropic layer thickness, length and semi-vertex angle.

References

1. Bagheri H., Kiani Y., Eslami M.R., 2017, Free vibration of conical shells with intermediate ring support, *Aerospace Science and Technology*, **69**, 321-332
2. Chopra I., Sirohi J., 2013, *Smart Structures Theory*, Chapter 6, Cambridge University Press
3. Civalek O., 2006, Free vibration analysis of composite conical shells using the discrete singular convolution algorithm, *Steel and Composite Structures*, **6**, 4, 353
4. Dapino M.J., Calkins F.T., Flatau A.B., 1999, Magnetostrictive devices, [In:] *Wiley Encyclopedia of Electrical and Electronics Engineering*, J.G. Webster (Edit.), John Wiley and Sons, Inc.
5. Engdahl G., 2000, *Handbook of Giant Magnetostrictive Materials*, Chapter 2, Academic Press
6. Firouz-Abadi R.D., Rahmanian M., Amabili M., 2014, Free vibration of moderately thick conical shells using a higher order shear deformable theory, *Journal of Vibration and Acoustics*, **136**, 5, 051001
7. Ghorbanpour Arani A., Khoddami Maraghi Z., Khani Arani H., 2017, Vibration control of magnetostrictive plate under multi-physical loads via trigonometric higher order shear deformation theory, *Journal of Vibration and Control*, **23**, 19, 3057-3070
8. Goodfriend M., Shoop K., Hansen T., 1994, Applications of magnetostrictive Terfenol-d, *Proceedings of Actuator 94, 4th International Conference on New Actuators*, Bremen, Germany
9. Hong C.C., 2014, Rapid heating induced vibration of circular cylindrical shells with magnetostrictive functionally graded material, *Archives of Civil and Mechanical Engineering*, **14**, 4, 710-720
10. Hong C.C., 2016, Rapid heating-induced vibration of composite magnetostrictive shells, *Mechanics of Advanced Materials and Structures*, **23**, 4, 415-422
11. Hunt F.V., 1953, *Electroacoustics: The Analysis of Transduction and its Historical Background*, American Institute of Physics for the Acoustical Society of America
12. Irie T., Yamada G., Tanaka K., 1984, Natural frequencies of truncated conical shells, *Journal of Sound and Vibration*, **92**, 3, 447-453
13. Jin G., Ma X., Shi S., Ye T., Liu Z., 2014, A modified Fourier series solution for vibration analysis of truncated conical shells with general boundary conditions, *Applied Acoustics*, **85**, 82-96
14. Kamarian S., Salim M., Dimitri R., Tornabene F., 2016, Free vibration analysis of conical shells reinforced with agglomerated carbon nanotubes, *International Journal of Mechanical Sciences*, **108**, 157-165

15. Kumar J.S., Ganesan N., Swarnamani S., Padmanabhan C., 2004, Active control of simply supported plates with a magnetostrictive layer, *Smart Materials and Structures*, **13**, 3, 487-492
16. Lam K.Y., Hua L., 1997, Vibration analysis of a rotating truncated circular conical shell, *International Journal of Solids and Structures*, **34**, 17, 2183-2197
17. Lam K.Y., Hua L., 1999, On free vibration of a rotating truncated circular orthotropic conical shell, *Composites, Part B: Engineering*, **30**, 2, 135-144
18. Lee S.J., Reddy J.N., 2004, Vibration suppression of laminated shell structures investigated using higher order shear deformation theory, *Smart Materials and Structures*, **13**, 5, 1176
19. Li F.M., Kishimoto K., Huang W.H., 2009, The calculations of natural frequencies and forced vibration responses of conical shell using the Rayleigh-Ritz method, *Mechanics Research Communications*, **36**, 5, 595-602
20. Mehditabar A., Rahimi G.H., Fard K.M., 2018, Vibrational responses of antisymmetric angle-ply laminated conical shell by the methods of polynomial based differential quadrature and Fourier expansion based differential quadrature, *Applied Mathematics and Computation*, **320**, 580-595
21. Nasihatgozar M., Khalili S.M.R., 2019, Vibration and buckling analysis of laminated sandwich conical shells using higher order shear deformation theory and differential quadrature method, *Journal of Sandwich Structures and Materials*, **21**, 4, 1445-1480, DOI: 10.1177/1099636217715806
22. Oates W.S., Smith R.C., 2008, Nonlinear optimal control techniques for vibration attenuation using magnetostrictive actuators, *Journal of Intelligent Material Systems and Structures*, **19**, 2, 193-209
23. Pradhan S.C., 2005, Vibration suppression of FGM shells using embedded magnetostrictive layers, *International Journal of Solids and Structures*, **42**, 9-10, 2465-2488
24. Pradhan S.C., Reddy J.N., 2004, Vibration control of composite shells using embedded actuating layers, *Smart Materials and Structures*, **13**, 5, 1245-1257
25. Qatu M.S., 2004, *Vibration of Laminated Shells and Plates*, Elsevier
26. Rao S.S., 2007, *Vibration of Continuous Systems*, Chapter 15, John Wiley & Sons, Inc.
27. Reddy J.N., 2002, *Energy Principles and Variational Methods in Applied Mechanics*, Chapter 7, John Wiley & Sons
28. Reddy J.N., 2004, *Mechanics of Laminated Composite Plates and Shells: Theory and Analysis*, Chapters 3 and 8, CRC Press
29. Shakouri M., Kouchakzadeh M.A., 2017, Analytical solution for vibration of generally laminated conical and cylindrical shells, *International Journal of Mechanical Sciences*, **131**, 414-425
30. Sofiyev A.H., 2018, Application of the first order shear deformation theory to the solution of free vibration problem for laminated conical shells, *Composite Structures*, **188**, DOI: 0.1016/j.compstruct.2018.01.016
31. Sofiyev A.H., Kuruoglu N., 2018, Determination of the excitation frequencies of laminated orthotropic non-homogeneous conical shells, *Composites, Part B: Engineering*, **132**, 151-160
32. Sofiyev A.H., Zerin Z., Allahverdiev B.P., Hui D., Turan F., Erdem H., 2017, The dynamic instability of FG orthotropic conical shells within the SDT, *Steel and Composite Structures*, **25**, 5, 581-591
33. Tong L., 1994, Free vibration of laminated conical shells including transverse shear deformation, *International Journal of Solids and Structures*, **31**, 4, 443-456
34. Xie K., Chen M., Li Z., 2017, An analytic method for free and forced vibration analysis of stepped conical shells with arbitrary boundary conditions, *Thin-Walled Structures*, **111**, 126-137
35. Zhang Y., Zhou H., Zhou Y., 2015, Vibration suppression of cantilever laminated composite plate with nonlinear giant magnetostrictive material layers, *Acta Mechanica Solida Sinica*, **28**, 1, 50-61

Manuscript received August 3, 2018; accepted for print May 27, 2019